Developmental Cell, Volume *56*

Supplemental information

Discrete *cis*-acting element regulates developmentally timed gene-lamina relocation and neural progenitor competence *in vivo*

Tanguy Lucas, Terry L. Hafer, Harrison G. Zhang, Natalia Molotkova, and Minoree Kohwi

Supplemental information

Discrete cis-acting element regulates developmentally timed gene lamina relocation and neural progenitor competence in vivo

T. Lucas, T.L. Hafer, H.G. Zhang, N. Molotkova and M. Kohwi

Correspondence to: mk3632@columbia.edu

This PDF file includes:

Table S1. Primers used to generate *hb* DNA FISH probe. Related to Figures 2 and 5.

Forward primer	Reverse primer
GAGGCTGCCGCTTGATTAACAC	ATCCAAGCAGGATCTCAGTAGC
AGGCTACTGAGATCCTGCTTGG	GCGTGGTTTGCTGTGGGAAATG
AAACGTGCCCTCCTGTTAAGTG	TAGATGGGCGGATATGGGTCTC
TCGAGTTCATCCCTCAACCTCC	GACAACAATTCCACTCAGCCAC
TGGCTGAGTGGAATTGTTGTCG	TCCTCCTTTCCCAGCTATTGAC
AGTCAATAGCTGGGAAAGGAGG	AGATGTGAGCCCAGTGTAATCC
GGGCAACTTTAAGCCCAGACAC	GGCATGGACTTTCGGCAATTAG
TCCAACATTACGCAGTACGCAG	CACTATTGTTTGGCCGCATAGC

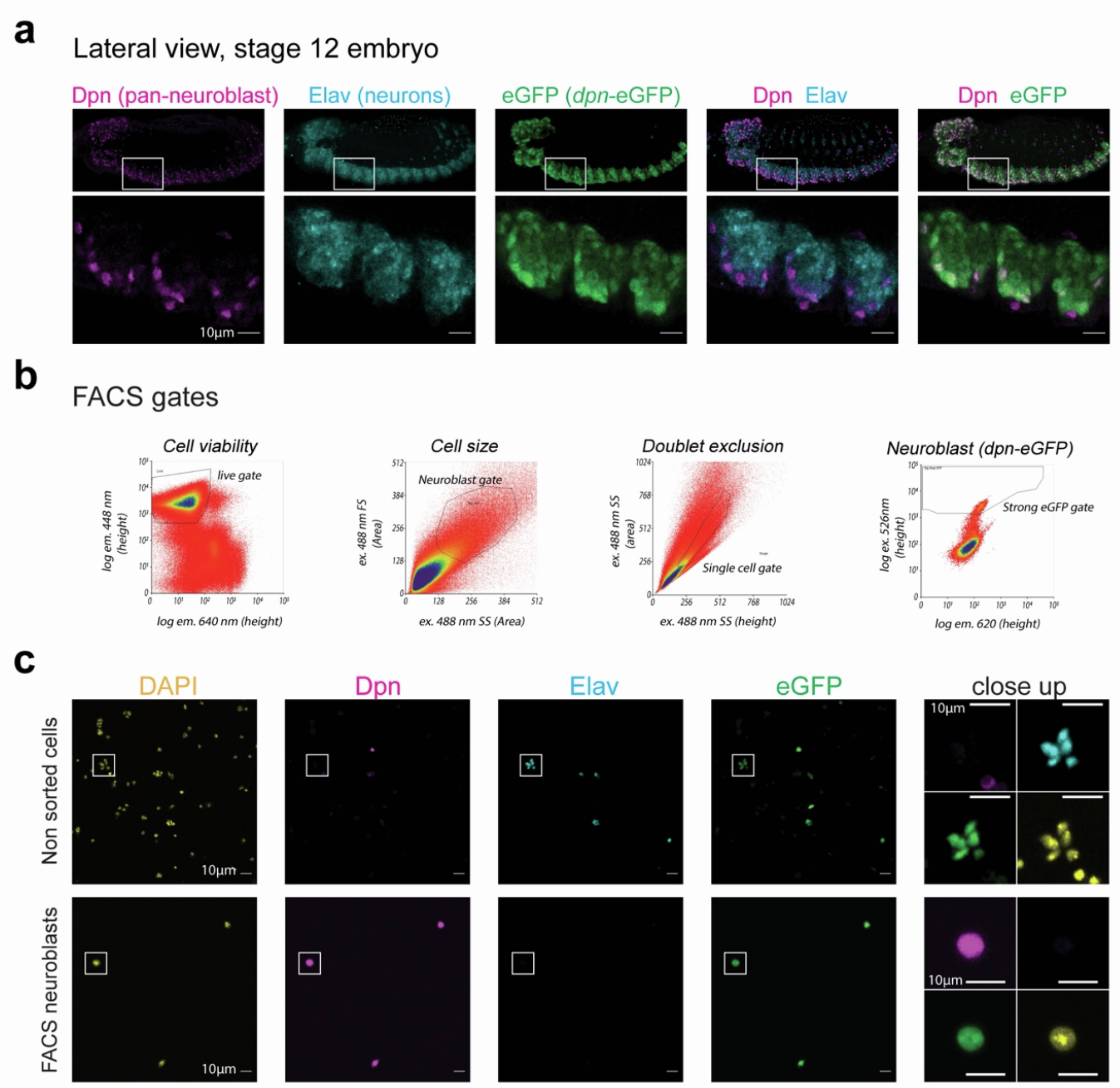

Supplemental Figure 1 (related to Figure 1). Neuroblast reporter and FACS validation.

a, Lateral views of stage 12 *dpn*-eGFP embryos immunostained for neuroblast marker, Dpn, neuronal marker, Elav, and GFP. Bottom panels show high magnification of inset. GFP is strong in neuroblasts but can be detected at lower levels in the neural progeny due to GFP perdurance. **b,** FACS scatter plots showing gates used to purify neuroblasts. Cell viability based on Calcein violet (viable) and 7AAD (dead) stains. **c,** Representative images of non-sorted cells (*top*) and sorted neuroblasts (*bottom*) stained with GFP, Dpn, and Elav. *Right*: high magnification of insets.

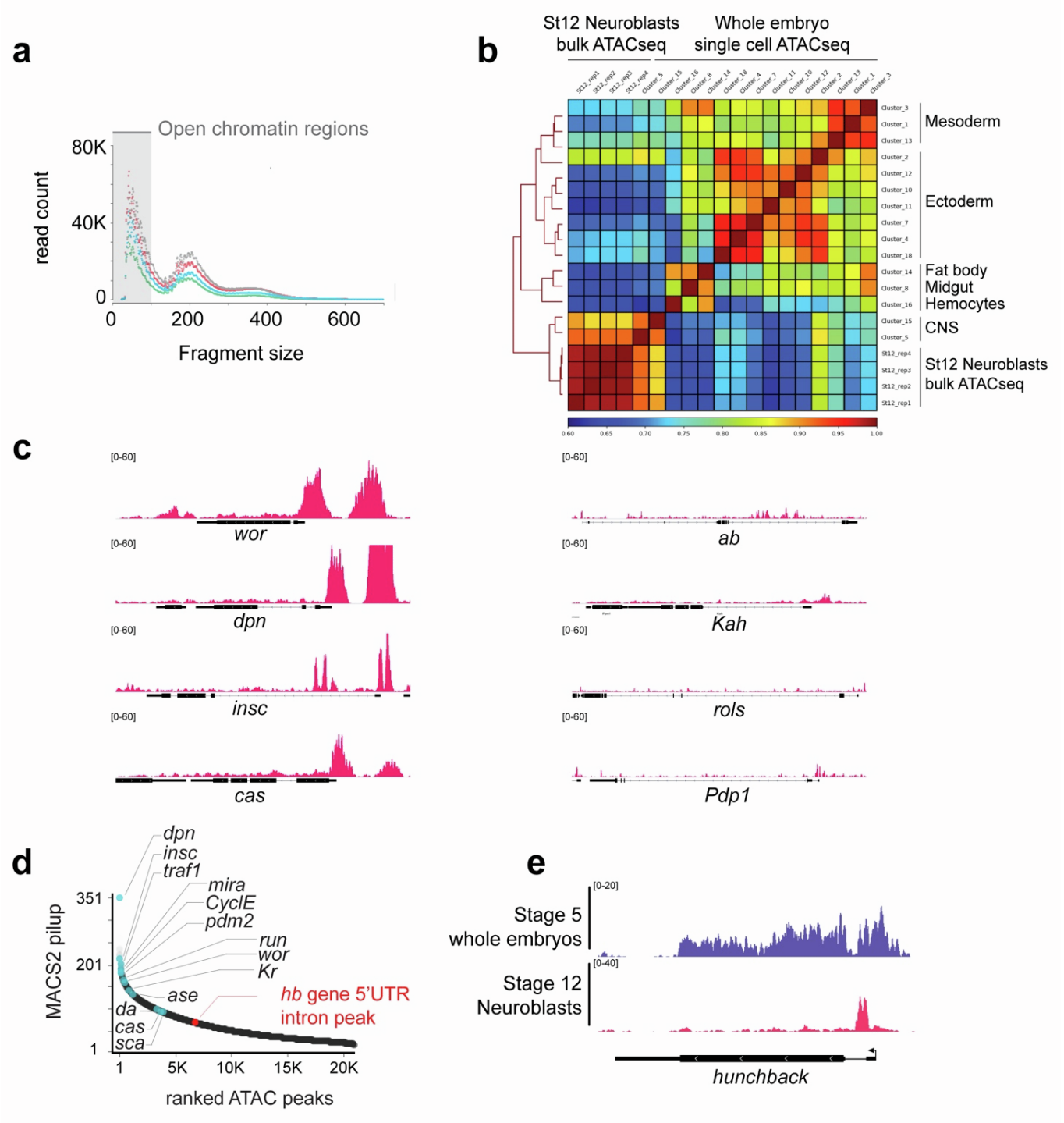

Supplemental Figure 2 (related to Figure 1): Validation of neuroblast-specific ATAC-seq data.

a, Distribution of fragment length from ATAC-seq libraries from four biological replicates of stage 12 FACS sorted neuroblasts. Open region peak (0-100bp), mono- nucleosome peak (150-250bp) and di-nucleosome peak (350-450bp) are visible. **b,** Pearson correlation heat map between stage 12 neuroblast ATAC-seq replicates (this paper) and all clusters from single cell ATAC- seq of whole, mid-embryogenic embryos (Cusanovich et al., 2018). **c,** ATAC-seq profile of example neuroblast genes (left) and non-neuroblast genes (right). **d,** ATAC peaks displayed ranked by amplitude (read pileup). A subset of neural genes expressed at stage 12 mid-embryogenesis is indicated along the distribution. **e,** reads per million normalized ATAC-seq profile spanning the *hb* locus at the cellular blastoderm Stage 5 (2-3h after egg laying, AEL) and the mid-embryogenesis Stage 12 (7-9h AEL). The *hb* locus is located on chromosome 3R.

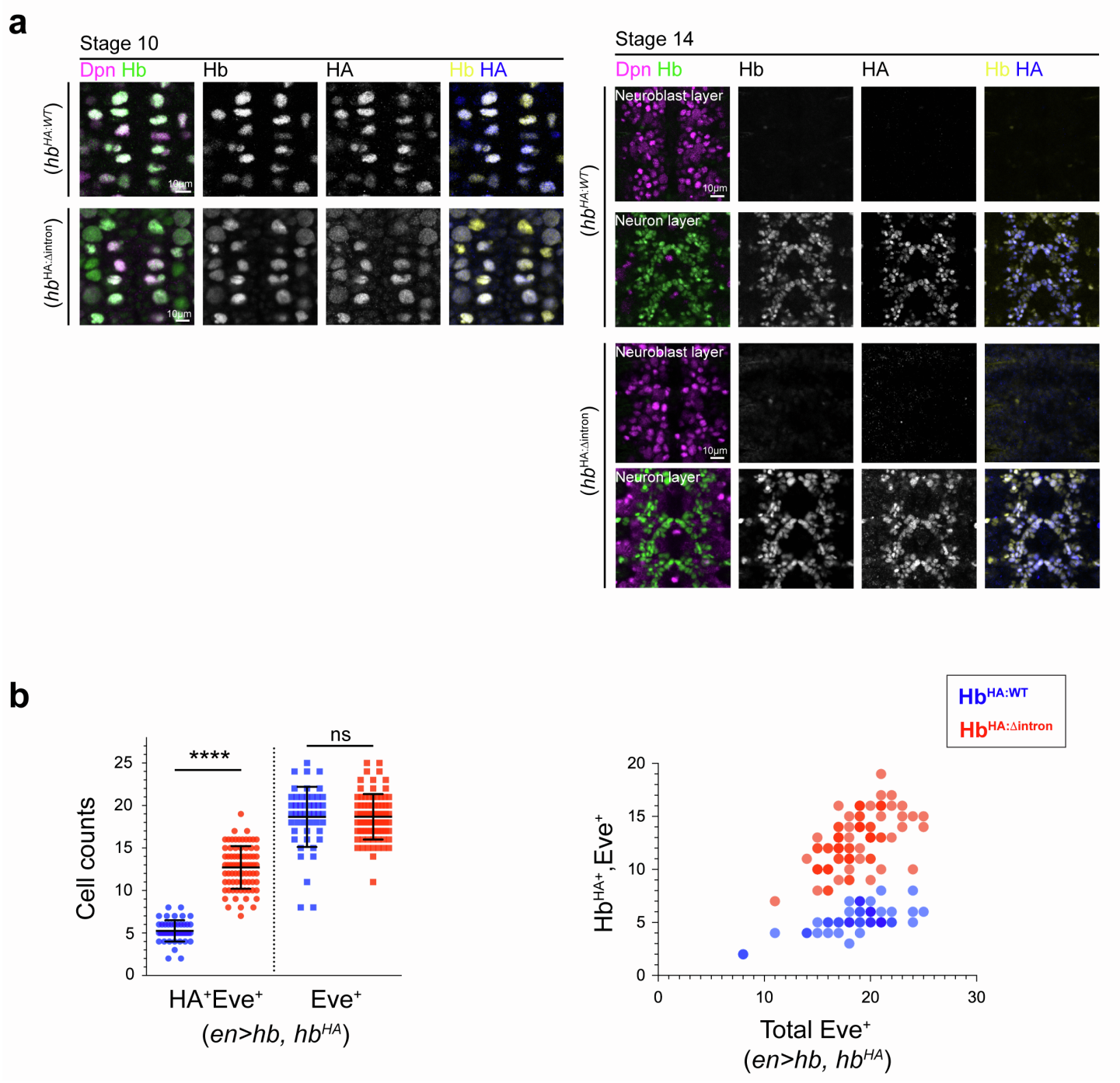

Supplemental Figure 3 (related to Figures 1 and 2): a, ventral nerve cord views of stage 10 and stage 14 $Hb^{HA:WT}$ and $Hb^{HA:\Delta intron}$ embryos immunostained with neuroblast marker, Dpn, Hb (all Hb protein), and HA (epitope for Hb protein derived only from BAC transgene). **b,** Quantified length of the early competence window for genotypes shown in a. *Left*: average length of early competence window (HA^+Eve^+) and total Eve cell number (Eve^+) in $Hb^{HA:WT}$ (blue) versus $Hb^{HA:\Delta intron}$ (red) genetic backgrounds. Data are represented as mean ± SD. *Right*: Corresponding scatter plots showing the number of Hb^{HA+} neurons relative to the number of Eve^+ cells in each NB7-1 lineage analyzed.

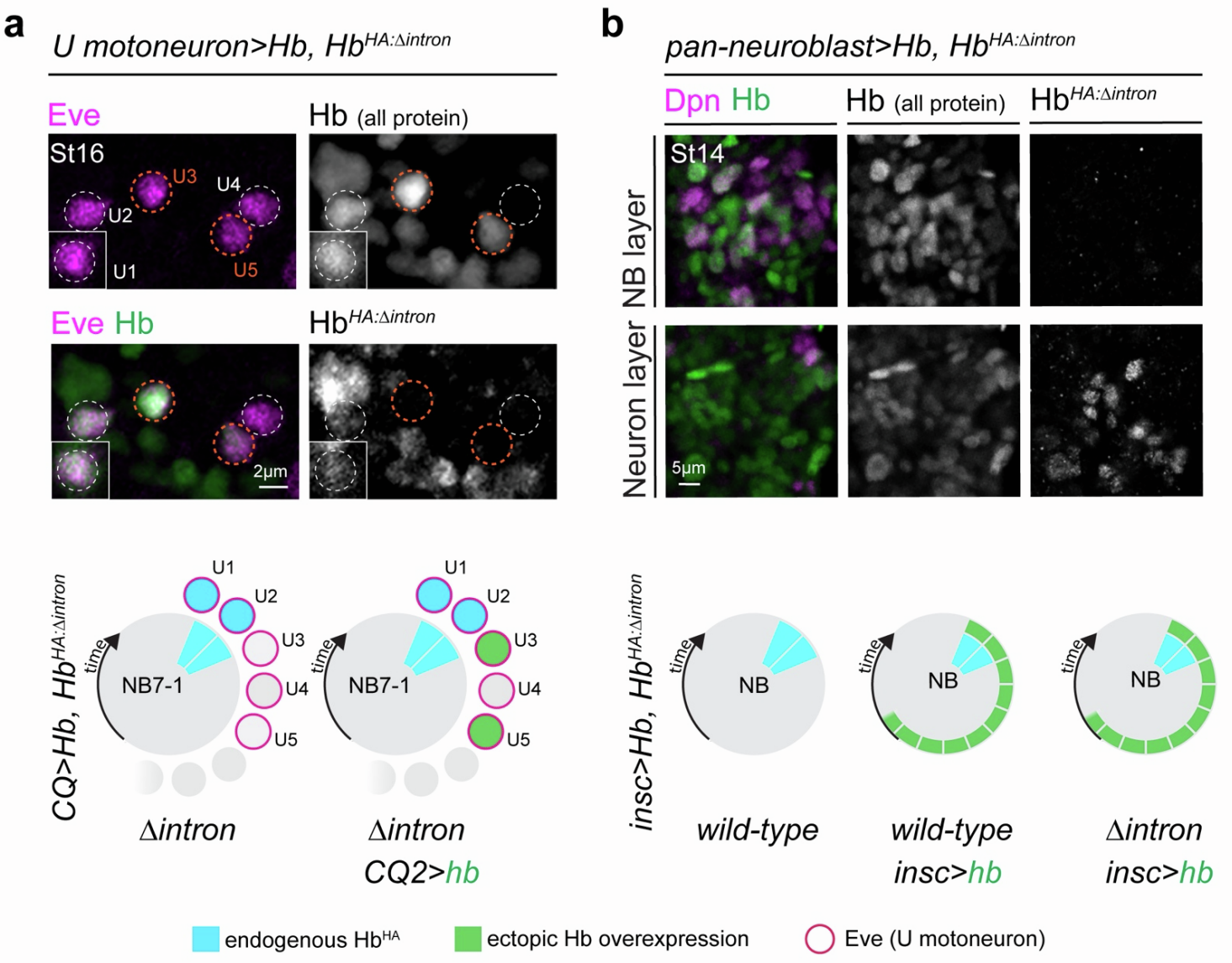

Supplemental Figure 4 (related to Figure 2): Exogenous Hb cannot induce Hb$^{HA:\Delta intron}$ directly within postmitotic neurons or within neuroblasts.

a, Stage 16 embryos stochastically misexpressing exogenous Hb (*cq2-gal4*, *UAShb*) in U-motoneurons (Eve^{+}) in the Hb$^{HA:\Delta intron}$ genetic background, immunostained for Eve, Hb and HA. Hb staining identifies late-born neurons (U3-U5) misexpressing Hb ectopically (see U3 and U5, orange dotted circles), HA staining identifies endogenous-Hb expression. **b,** Stage 14 embryos overexpressing Hb in all neuroblasts (*insc-gal4*, *UAShb*) in the Hb$^{HA:\Delta intron}$ background, immunostained for Dpn, Hb and HA. The neuroblast layer (top) and neuron layer (bottom) from a single hemisegment is shown. Schematic summaries are shown below each panel.

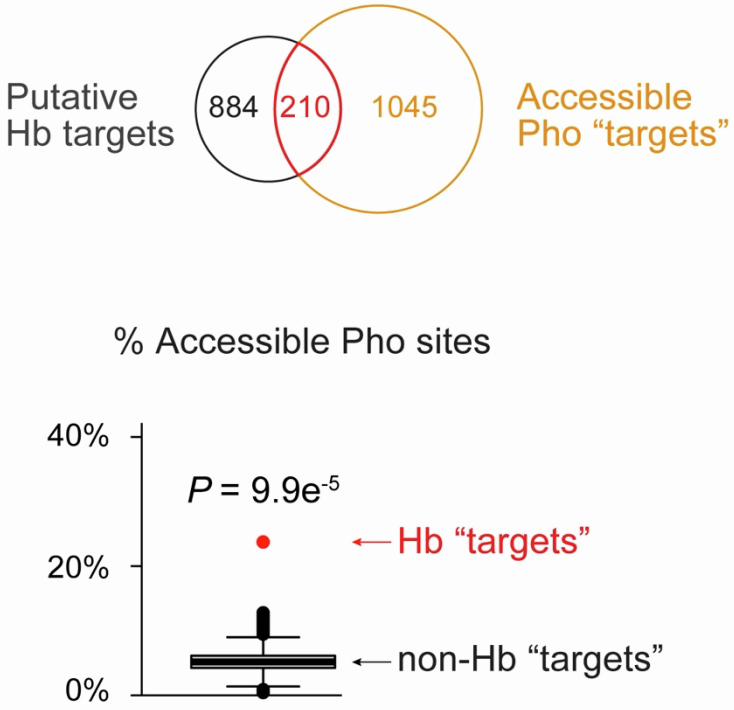

Supplemental Figure 5 (related to Figure 4).

Putative Hb targets which are genes in close proximity to Hb binding loci in the embryonic CNS (Sen et al., 2019) are found to be enriched for chromatin accessible Pho binding motifs in stage 12 neuroblasts compared to non-Hb targeted loci.

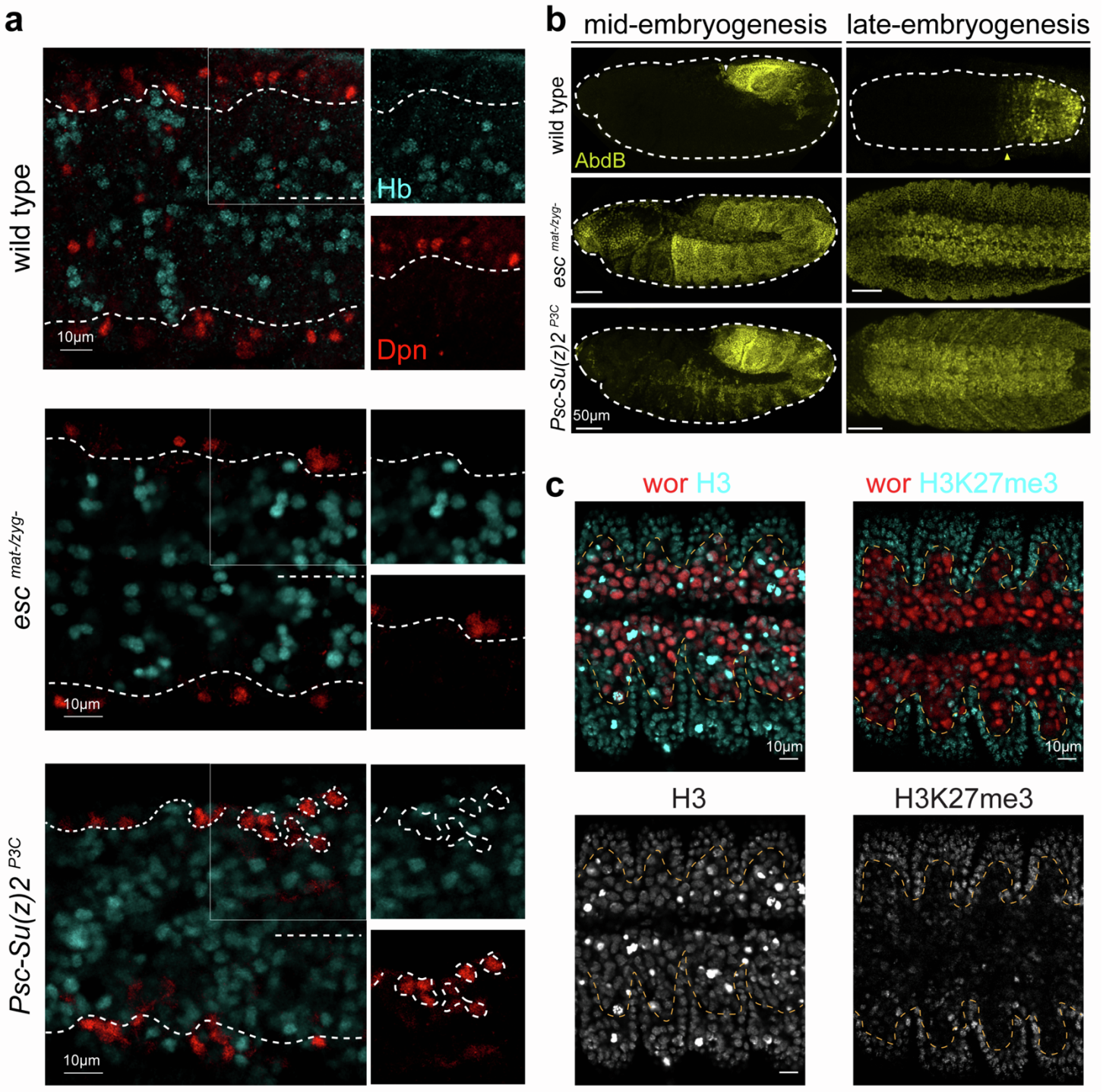

Supplemental Figure 6 (supplement to Figure 5): *hb* is not derepressed in strong PcG mutant alleles.

a, Ventral view of the VNC stained with Hb and neuroblast marker, Dpn in WT, maternal and zygotic *esc* mutant, and Psc-Su(z)2 (P3C) double mutant background (midline, straight dashed line; VNC border, curvy dashed line). Dpn and Hb channels of insets are shown individually at the right. **b,** *Left:* Abd-B expression in lateral view, mid-embryogenic embryos (dorsal, down). *Right:* ventral view of late-stage embryos. **c,** *Top:* total histone, H3, or PcG-associated mark, H3K27me3, immunostained with pan-neuroblast marker, Worniu (Wor) in stage 14 WT embryos. Gray scale image shows histone channel alone. Orange dashed line shows VNC border. Anterior is to the left in all panels.

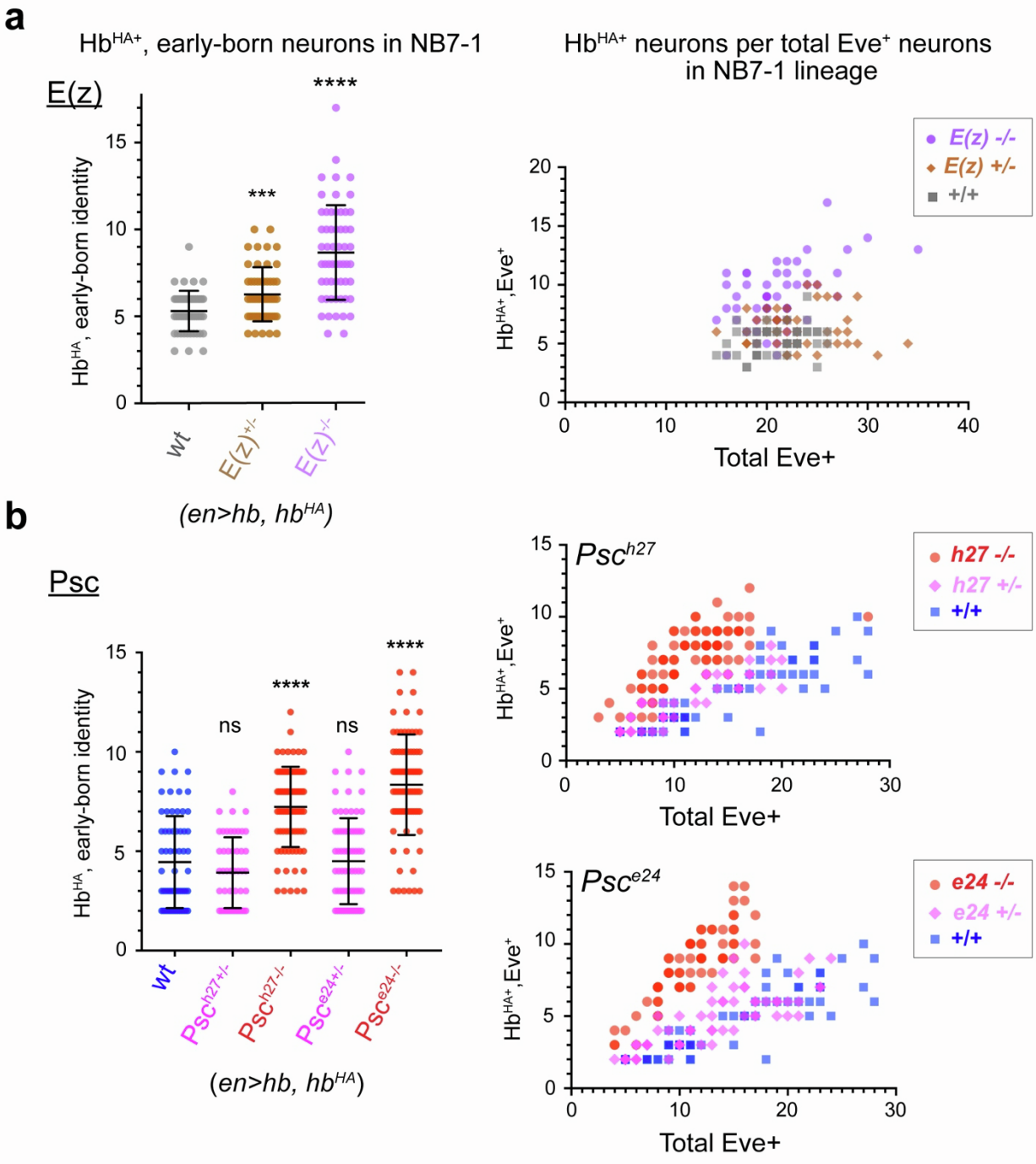

Supplemental Figure 7 (related to Figure 6): Scatter plots for early competence window in *E(z)* and *Psc* and mutants.

a, *Left*: Average early competence window. *Right*: Scatter plots showing the number of Hb^{HA+} neurons relative to the number of Eve^{+} cells in each NB7-1 lineage analyzed. **b,** *Left*: Average early competence window. Two Psc null alleles (Psc^{h27} and Psc^{e24}) are shown. Scatter plots shown to the right. All data are represented as mean ± SD.